Various Modes of Faulting Associated with Mid-Ocean Ridges: Cleft Segment

Elizabeth Watkins and Dr. Leslie Sautter

Department of Geology and Environmental Geosciences, College of Charleston

Abstract

To explain the modes of faulting that characterize the Cleft Segment of the Juan de Fuca mid-ocean ridge, a combination of fault mode models would be needed to account for the dynamic geologic setting. Bathymetric profiles from multibeam sonar data were taken perpendicular to the spreading axis of the Northern, Central, and Southern Cleft areas, and ridge spacing with associated depths and the overall ridge flank slopes were calculated. The Northern Cleft is asymmetric in ridge depth and distance from the axis, as well as in the overall slopes of the East and West flanks; however, the opposite is observed moving toward the Southern Cleft. Fault characteristics in the cross sections were used in combination with hydrothermal surface features to interpret the various faulting modes of the study area. Northern Cleft is stretching-dominated while Southern Cleft is buoyancy-dominated in faulting.

Methods

- A bathymetric survey was conducted by University-National Oceanographic Laboratory System's (UNOLS) Woods Hole Oceanographic Institution from August 2014-September 2014.
- A Kongsberg EM122 multibeam echosounder aboard the R/V *Atlantis* was used to collect bathymetry and backscatter intensity data data.
- 2D and 3D bathymetric, backscatter, and slope aspect surfaces were created using CARIS HIPS and SIPS 9.0 and BASE Editor.
- Profiles were created perpendicular to the spreading axis and extend 20,000 m to the east and west from the spreading center to see relief and calculate overall faulted ridge spacing from the ridge axis.
- Faulted ridge distance from the axis on the East and West sides were graphed in relation to the faulted ridge depths using the profiles.
- The overall slope of each profile was derived using the faulted ridge distance from the axis and ridge depths data.

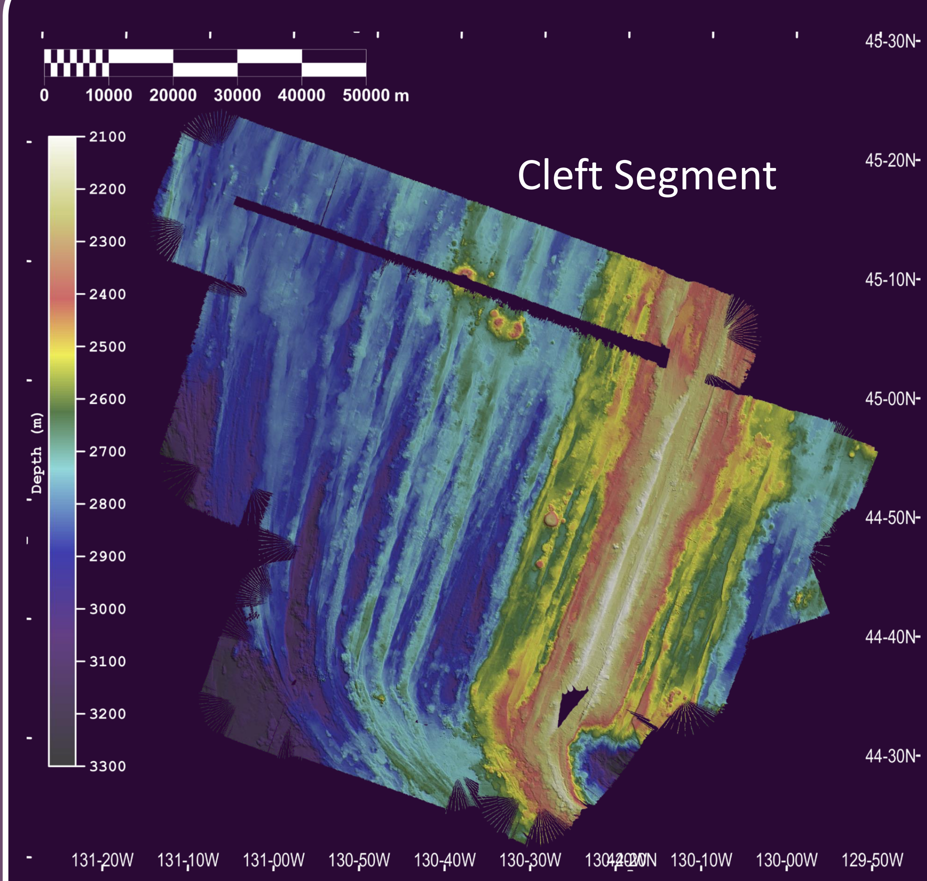

Figure 1. 20 m and 50 m combined CUBE surface of the study area, Cleft Segment of the Juan de Fuca Ridge.

Location of Study

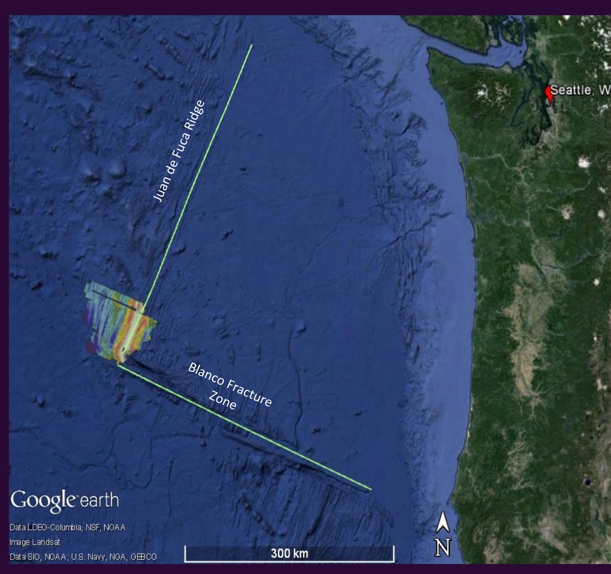

Figure 2. Cleft Segment is located at the southern end of the Juan de Fuca Ridge approximately 500 km off the coast of Washington (CUBE surface on Google Earth image).

Background

The Juan de Fuca Plate is the smallest of Earth's tectonic plates and is bounded by all three types of dynamic plate boundaries. The Juan de Fuca Ridge (JDFR), the Western boundary of the Juan de Fuca Plate, stretches a length of 500 km and has an intermediate spreading rate of 56 mm per year; more than twice as fast as the Mid-Atlantic Ridge, which is ~30 times the length of JDFR (Cordier et al., 2012). JDFR is divided into 7 main ridge segments. This study focuses on the southern-most spreading ridge segment of the JDFR—Cleft Segment. Cleft Segment, 80 km in length, is bounded by the Blanco Fracture Zone to the south and the Vance Segment to its north (Embley et al., 1991).

Modes of faulting are highly variable and are defined by an area's morphology, buoyancy, and hydrothermal processes (Buck, 2005). Extensive studies of Cleft Segment conducted in the 1980s are considered a benchmark for bathymetric surveying quality. They revealed extensive morphologic and volcanic characteristics, evidence of hydrothermal features and massive eruptions along the segment (Embley et al., 1991).

Using the techniques defined in the 1980's studies, various types of features can be identified. The physiographic characteristics exhibited on the West and East side of the Cleft Segment can be used in combination with the identified features to interpret the fault behavior along the ridge as well as other hydrothermal processes and systems associated with the Cleft Segment.

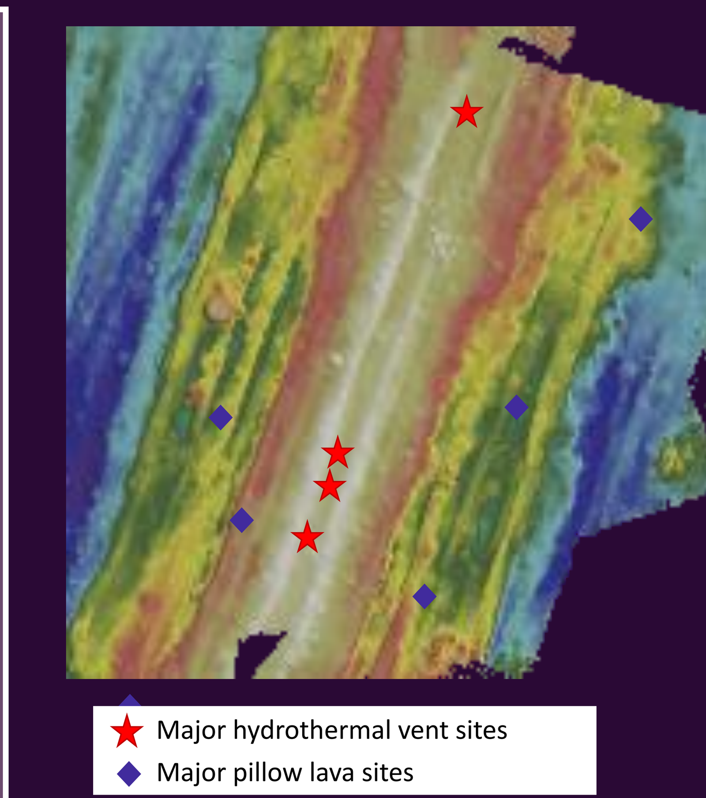

Figure 3. Location of major hydrothermal vent sites and areas characterized by significantly large pillow lava mounds (Embley et al., 1991).

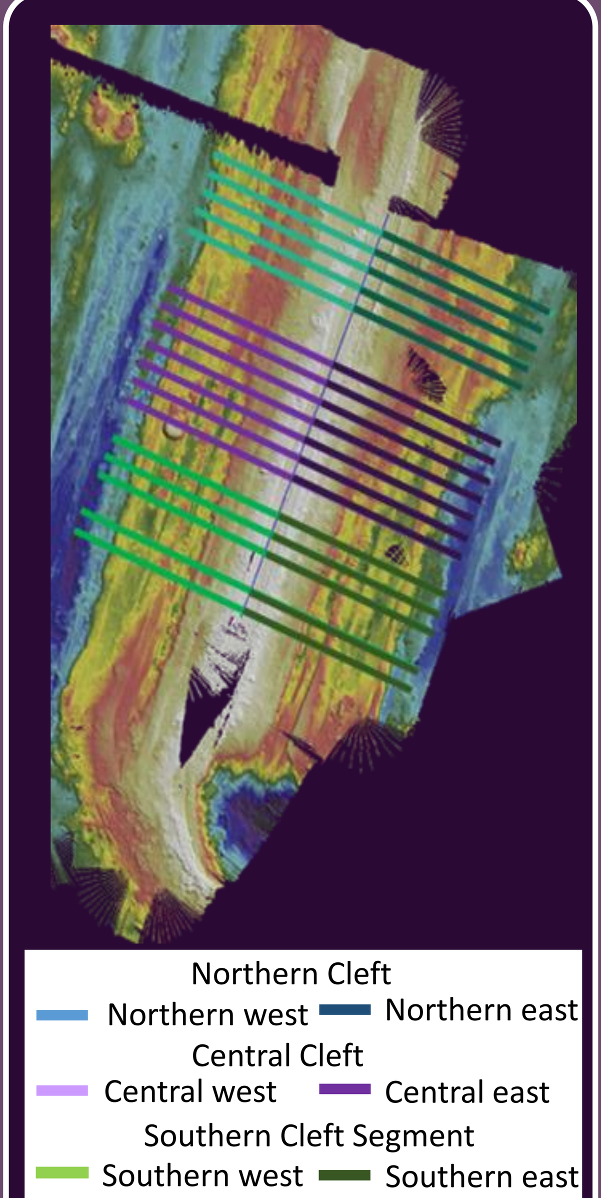

Figure 4. Profile locations delineating the Northern, Central, and Southern sections of the Cleft Segment. The darker portions of the profile lines represent the East side of the spreading ridge.

Northern Cleft

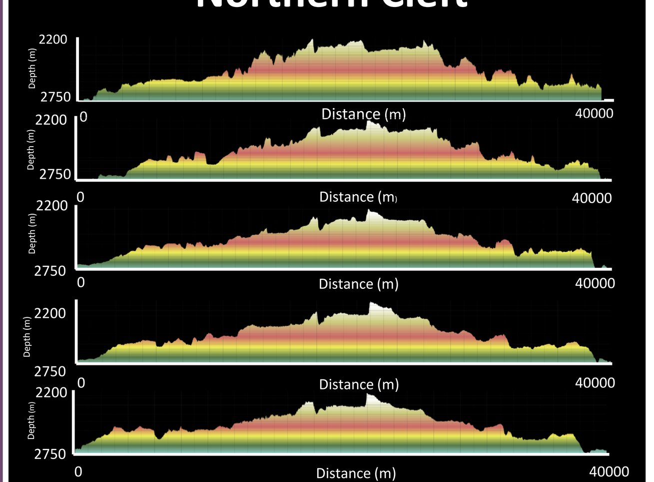

Figure 5a. Profile cross-sections along the Northern Cleft section.

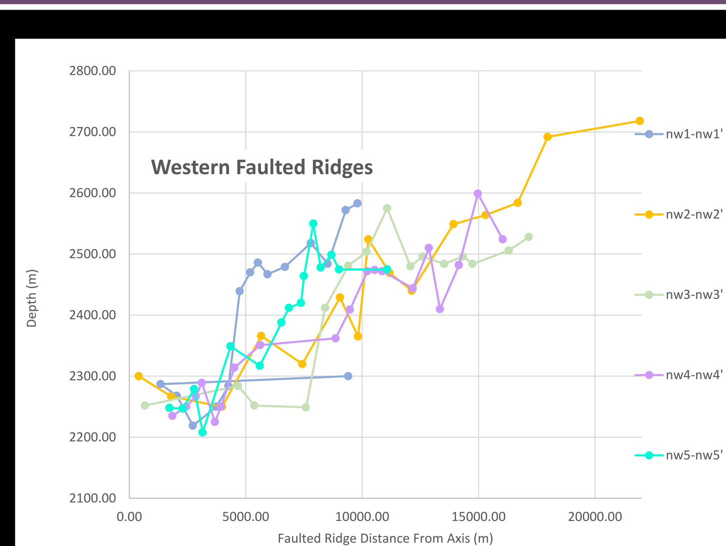

Figure 5b. Distance of western faulted ridges of Northern Cleft from the spreading axis in relation to their depth.

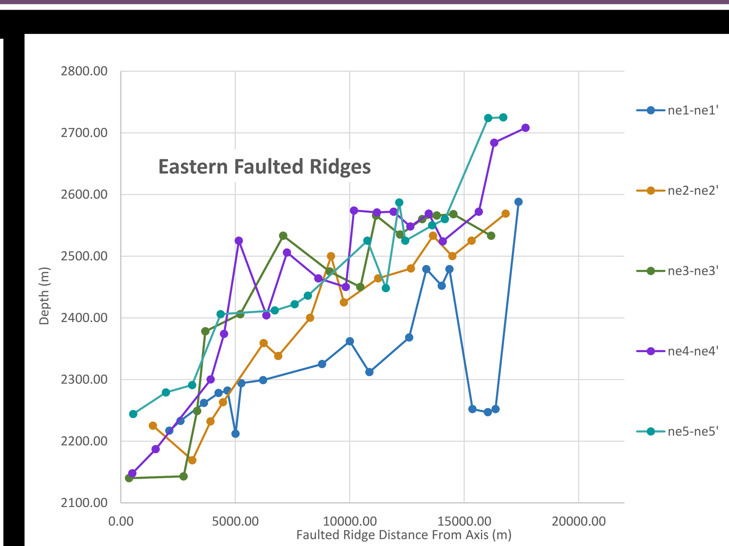

Figure 5c. Distance of eastern faulted ridges of Northern Cleft from the spreading axis in relation to their depth.

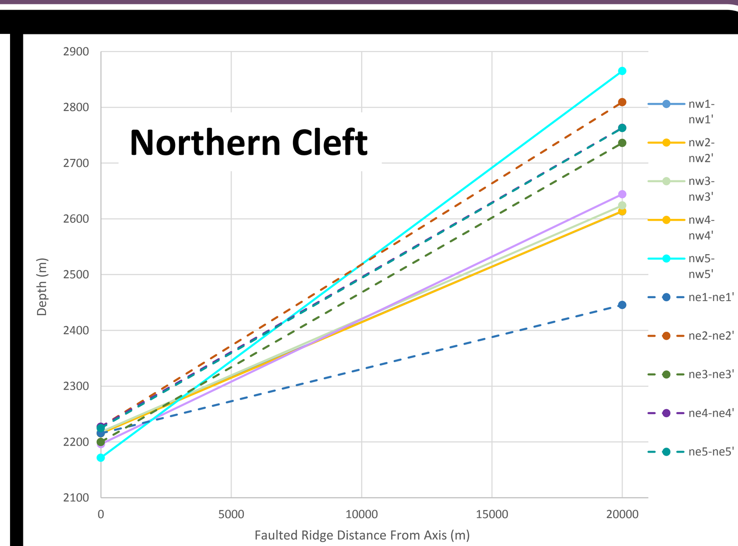

Figure 5d. Northern Cleft overall slope associated with each faulted axis-ridge distance in relation to their depth from both the western (solid lines) and eastern (dashed) profiles.

Central Cleft

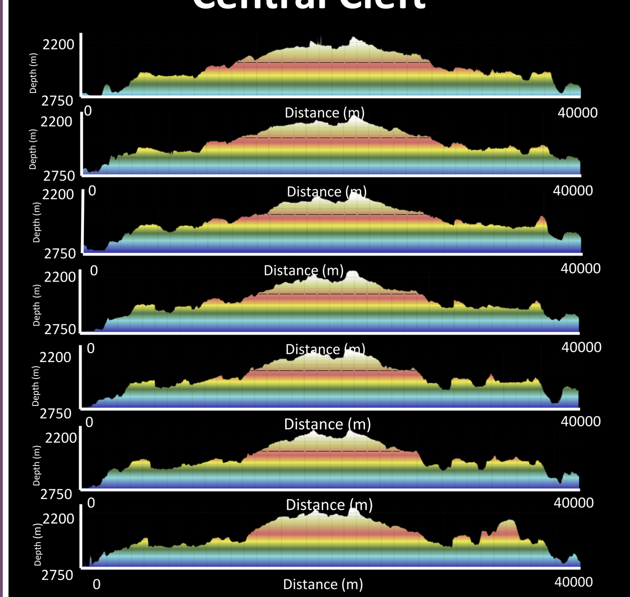

Figure 6a. Profile cross-sections along the Central Cleft section.

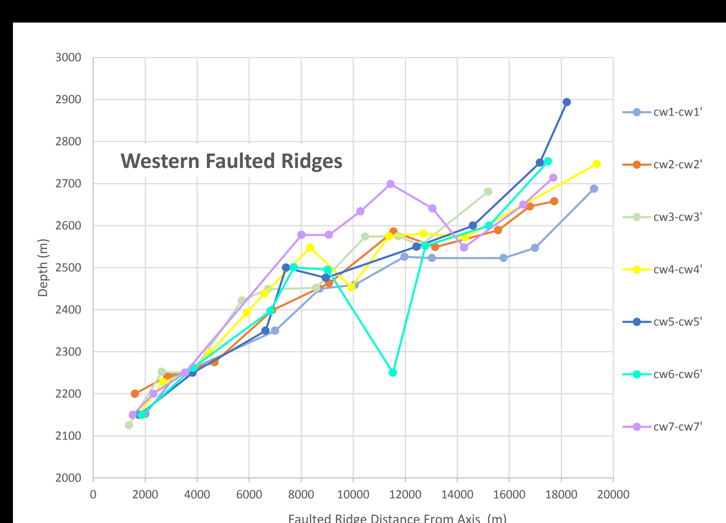

Figure 6b. Distance of western faulted ridges of Central Cleft from the spreading axis in relation to their depth.

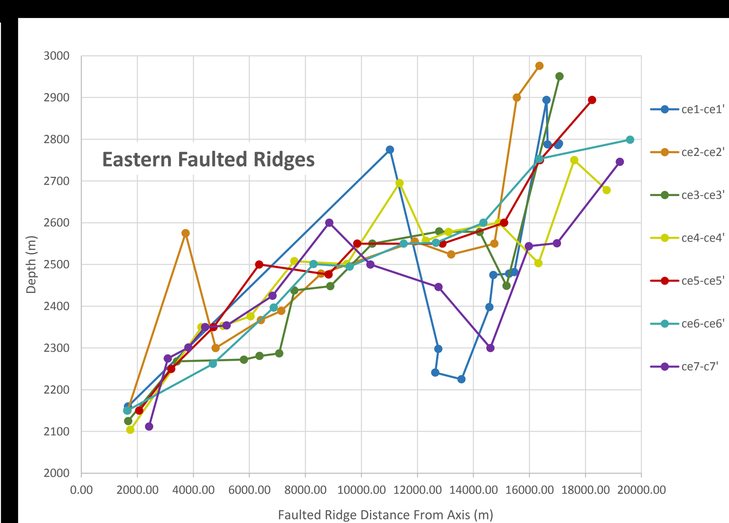

Figure 6c. Distance of eastern faulted ridges of the Central Cleft from the spreading axis in relation to their depth.

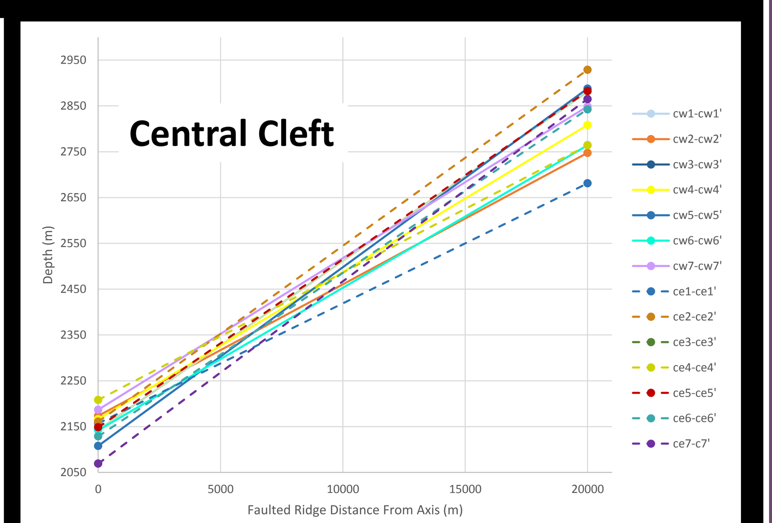

Figure 6d. Central Cleft overall slope associated with each faulted axis-ridge distance in relation to their depth from both the western (solid lines) and eastern (dashed) profiles.

Southern Cleft

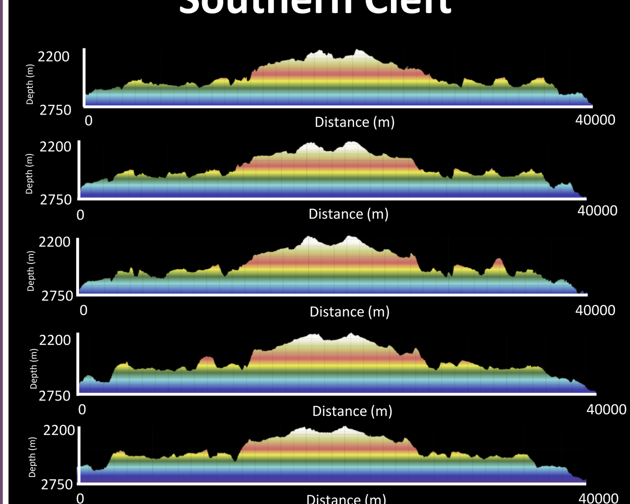

Figure 7a. Profile cross-sections along the Southern Cleft section.

All profiles: VE=5x

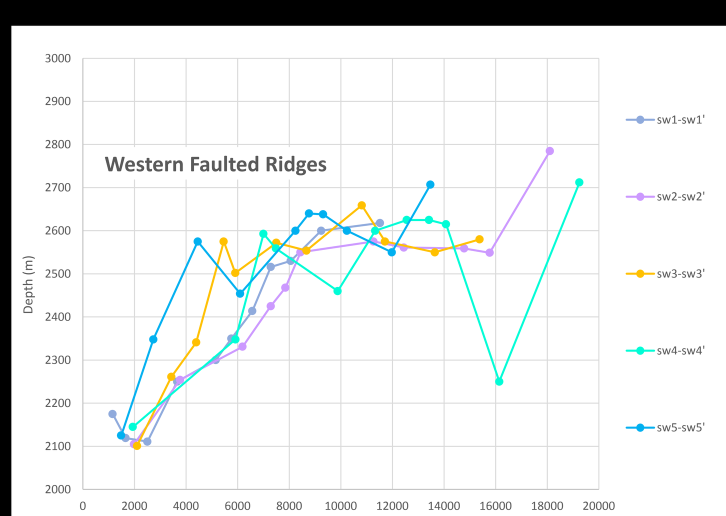

Figure 7b. Distance of western faulted ridges Southern Cleft from the spreading axis in relation to their depth.

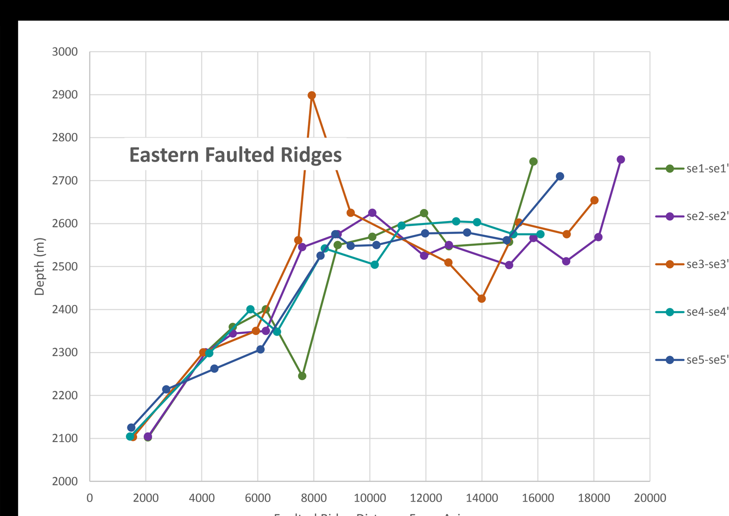

Figure 7c. Distance of eastern faulted ridges of Southern Cleft from the spreading axis in relation to their depth.

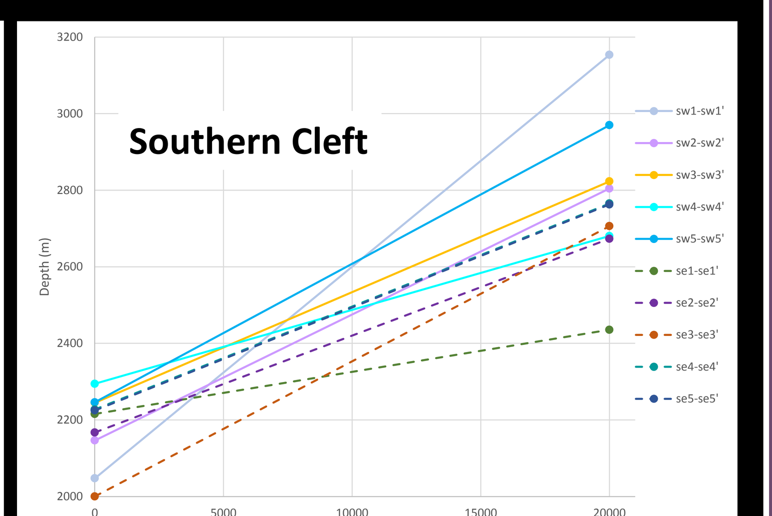

Figure 7d. Southern Cleft overall slope associated with each faulted axis-ridge distance in relation to their depth from both the western (solid lines) and eastern (dashed) profiles.

Results

- Depth range of the profiles increases from north to south.
- The majority of the faulted ridges do not dip significantly towards or away from the axis. In very few cases, some faulted ridges seem to favor dipping towards the axis very slightly but never away. As a whole, the faulted ridges of each study area are oriented close to 90 degrees (Fig. 5a, 6a, 7a).
- The west vs. east faulted ridges of the Northern Cleft study area appear to be the least symmetric of the three study areas (Figs. 5a-d). The east side of the spreading ridge exhibits a steeper slope characterized by faulted ridges of varying height, while the west side faulted ridges appear in a more "staircase" or uniform way— becoming generally shorter with increasing distance from the spreading center.
- The Central Cleft study area exhibits faulted ridges that are also asymmetric from west to east; however, less dramatically than in the Northern area (Figs. 6a-d). The general slope of the west and east sides are fairly similar—there is no distinct difference in slope; however, it is still not the most symmetric of the studied areas.
- The most west-east symmetric faulted ridges are within the Southern Cleft area (Fig. 7a-d). This area is also the most symmetric regarding the overall slope of the east and west side.

Discussion and Conclusions

The Plate Tectonics-generated axial valley can be filled by magmatic dyke intrusion at lower stress than required for faults that occur to accommodate tension and slip. This standard model of faulting modes led scientists to assume that faults form only during periods when no magma is available for intrusion and the total slip on faults is entirely time-dependent regarding the dyking intrusion events (Buck, 2005). This standard model proposes that all faulted ridges result from stretching thin axial lithosphere during amagmatic periods. Cleft Segment, however, does not singularly fit this standard model of faulting nor any of the models created recently. The Northern, Central, and Southern Cleft study areas individually display the processes and modes of faulting that encompass Cleft Segment as a whole.

Northern Cleft exhibits asymmetric high angle faulting. Small-offset, high angle faults west of the axis (Figure 5a), are found where magmatic accretion is most likely occurring. Diking processes play a large role in this fault mode. Hydrothermal vents are known to be present in the axial valley (Fig. 3) and are a proxy for intrusive diking. Buck (2005) inferred that diking is 50% (M = 0.5) responsible for the faulting in this area, associated with the high angle, asymmetric faulting. These characteristics are consistent with and strongly indicate the presence of stretching-dominated faulted ridges at Northern Cleft.

Southern Cleft (Figs. 7a-d) is characterized by west-east symmetry, steeper slopes, and a greater depth range than to the north—indicating increased lithospheric thinning at the axis (Cordier et al., 2012). These associated characteristics of the Southern Cleft area are consistent with those of buoyancy-dominated faulted ridges. Central Cleft displays the transition from the Northern Cleft stretching-dominated faulted ridges to the Southern Cleft buoyancy-dominated faulted ridges (Fig. 6a-d).

In summary, Cleft Segment exhibits both stretching-dominated, buoyancy-dominated modes of faulting as well as intermediate modes. Hydrothermal processes and the tectonic forces associated with the geologic setting are likely the cause of geomorphic variation of this spreading ridge segment.

References

Buck, W. R. (2005). Modes of faulting at mid-ocean ridges. *Nature, 434*(7034), 719-723.

Cordier, C., Caroff, M., & Rannou, E. (2012). Timescale of open-reservoir evolution beneath the south Cleft segment, Juan de Fuca ridge. *Mineralogy & Petrology, 104*(1/2), 1-14. doi:10.1007/s00710-011-0159-5

Embley, R. W., and W. W. Chadwick Jr. (1994), Volcanic and hydrothermal processes associated with a recent phase of seafloor spreading at the northern Cleft segment: Juan de Fuca Ridge, J. Geophys. Res., 99(B3),4741–4760, doi:10.1029/93JB02038.

Acknowledgements

Special thanks to the College of Charleston BEAMS Program for the learning opportunity, Josh Mode holding a weekend workshop to introduce CARIS, CARIS for Academic Partnership, Department of Geology and Geosciences, College of Charleston School of Science and Mathematics, and contributing partners: NOAA, UNOLS, and Woods Hole Oceanographic Institution.

Lizzy Watkins
WatkinsLA@g.cofc.edu